Chapter 11 – NUMERICAL SOLUTIONS FOR THE CAWAPI CONFIGURATION ON UNSTRUCTURED GRIDS AT KTH/FOI, SWEDEN – PART II

by

Adam Jirásek[1] and Arthur Rizzi[2]

11.1 SUMMARY

This article represents a second contribution of the Swedish Defence Research Agency, FOI, and the Royal Institute of Technology, KTH, to the Cranked-Arrow Wing Aerodynamics Project International, CAWAPI. The main focus of this article is on evaluation of the effect of different formulation of boundary conditions on the engine mass flow and resulting wing upper surface pressures.

11.2 INTRODUCTION

This study is a part of CAWAPI international collaborative activities [11-1], [11-2] and complementary study to that of Goertz et al. [11-3] aiming at detailed testing of steady and non steady CFD analysis of an F-16XL fighter configuration. The detailed study of different turbulence models for steady and unsteady analysis of this configuration is in [11-3]. The study in this article focuses instead on formulation of boundary conditions in the inlet and engine exhaust face.

Figure 11-1 shows the CAWAPI configuration. It has two internal boundary conditions, one in the inlet and second at the mixing plane in the nozzle – see Figure 11-2.

Figure 11-1: CAWAPI F-16XL-1 Configuration at Higher Angle of Attack, NASA Photo, 1996.

[1] FOI R&D Engineer.

[2] Professor, Department of Aeronautics.

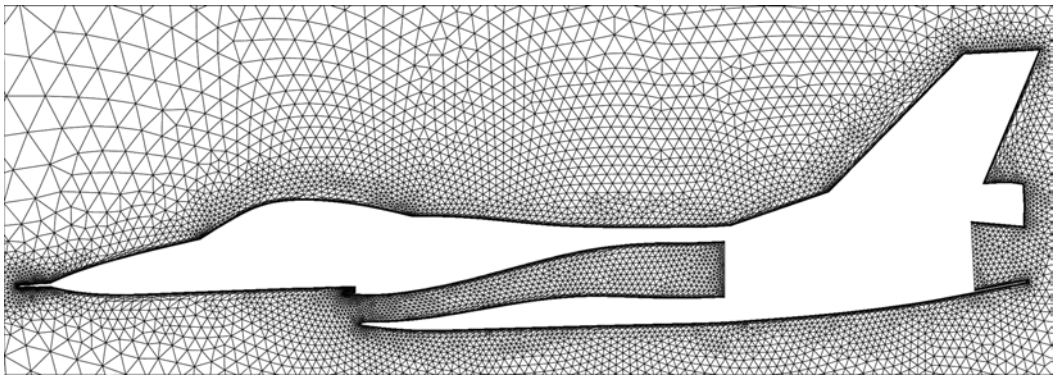

Figure 11-2: CAWAPI F-16XL-1 Configuration, Symmetry Plane of the Hybrid Grid Showing the Meshed Inlet Duct and Nozzle.

The boundary conditions applied at these boundaries were static pressure at the outlet boundary in inlet and total states inflow boundary at the mixing plane. The values of static pressure in inlet and total states in the nozzle were estimated using generic engine model and are given in Lamar et al. [11-1] – see Table 11-1.

Table 11-1: Propulsion Conditions as a Function of Flight Conditions

	Inlet Duct Exit Conditions			Mixing Plane Conditions		
FC	T_{stat}[K]	P_{stat}[Pa]	u [m/s]	Mach number	T_0 [K]	P_0 [Pa]
FC07	276.7	75,842	115.7	0.347	583.3	158,579
FC19	269.9	70,327	105.4	0.320	583.3	148,237
FC25	261.1	60,122	144.7	0.447	671.7	181,332
FC46	246.4	40,334	123.2	0.390	580.6	102,042
FC70	288.3	73,429	141.6	0.416	666.7	206,843
FC50	244.5	35,577	147.3	0.470	641.4	116,866
FC51	239.8	35,784	142.8	0.460	636.7	115,418

The estimate does not take to account a balance of the mass flow. Despite that most participants use those conditions. The only organization which uses different type of boundary conditions is USAFA [11-4].

The inspection of the result with OMS boundary conditions shows large discrepancy between the values of the mass flow through inlet and through nozzle, where the value of mass flow leaving the engine through mixing plane was substantially larger then the amount of mass flow entering the engine through inlet. The effect of this discrepancy as well as the influence of substantially larger value of mass flow leaving the engine is unknown. This chapter focuses on study of the possible effect of the formulation of the boundary conditions in the inlet and nozzle on flow around delta wing of the CAWAPI configuration.

11.3 FLOW SOLVER

The CFD flow solver used for this study is the Edge [11-5], a finite volume Navier-Stokes solver for unstructured meshes. It employs local-time-stepping, local low-speed preconditioning, multigrid and dual-time-stepping for steady-state and time-dependent problems. The data structure of the code is edge-based so that the code is constructed as cell-vertex. It can be run in parallel on a number of processors to efficiently solve large flow cases. It is equipped with a number of turbulence models based both on the eddy-viscosity and an explicit algebraic Reynolds stress model EARSM combined with Hellsten k-ω model [11-6]. The solver is also equipped with several boundary conditions; one of them enables control of a mass flow through inflow and outflow boundary and Mach number at the outflow boundary [11-7].

11.4 CALCULATIONS WITH ENGINE BOUNDARY CONDITIONS

11.4.1 Methodology

Three formulations of boundary conditions were used:

- First, static pressure in the inlet and total states in the missing plane with values given in Lamar et al. [11-1]. This case is a benchmark case. Detailed description can be found in Goertz et al. [11-3]. This setup is called benchmark case.
- Value of static pressure from Lamar et al. [11-1],[11-2] was kept in inlet and resulting value of mass flow was used in boundary conditions in the nozzle. The value of mass flow is updated in every step of the international process. Total temperature in the nozzle was taken from Lamar et al. [11-1],[11-2]. This setup is called on-line shearing.
- Mass flow boundary conditions in both the inlet and nozzle were used. The value of mass flow is frozen for entire calculations and is taken from the benchmark calculations as the value of the mass flow through inlet. Total temperature in the nozzle was taken from Lamar et al. [11-1],[11-2]. This setup is called constant mass flow.

In some cases change of the boundary conditions worsened convergence of the computational process. In order to evaluate its effect on solution the following methodology was employed. The solution is not considered in terms of the average values and deviation. The computational process is run for sufficiently large number of steps so that it would be usually considered a converged solution. From that point the computational process was run for additional number of steps, usually 20% of entire length of international process. During this additional time the solution is sampled approx 20 times. Then the final solution is expressed in values of mean and deviation. As an example take a C_p coefficient in every mesh point:

$$C_p = C_{p_0} \mp \Delta C_p$$

where mean is

$$C_{p_0} = \frac{1}{n}\sum C_p$$

and deviation

$$\Delta C_p = \frac{1}{n}\sum \left(C_{p_0} - C_p\right)^2$$

The deviation of a particular variable should not be seen as an artefact of time-unsteadiness of solution, since the solution is calculated as a steady one using technique improving convergence such as multi-grid and local-time-stepping. It should be instead taken as an uncertainty due to sampling of the steady-state CFD solutions.

11.4.2 Results

Three flight conditions are investigated in depth – FC46, FC19 and FC7. Of particular interest are changes of the pressure distribution on the upper side of the wing and the value of total pressure in the mixing plane which is necessary to balance the value of mass flow through inlet.

11.4.2.1 Flight Condition FC46

At this flight conditions, the discrepancy between the value of mass flow through the inlet and nozzle in benchmark case is about $\frac{\dot{m}_{Nozzle}}{\dot{m}_{Inlet}} \approx 2$. Since the total temperature in the mixing plane is kept constant, it is expected that the value of total pressure would be substantially lower. Interesting is the effect of formulating boundary conditions on the pressure distribution on the upper side of wing. The constant mass flow setup had a minor effect on solution. The value of total pressure is as expected lower and there are noticeable differences of solution in vicinity of the nozzle but most of solution remains unaffected. Contrarily to this the on-line shearing setup worsened convergence of the computational process and changed pressure distribution on the upper side of wing. Figure 11-3 shows the distribution of absolute values of $C_{p_{Benchmark}} - C_{p_{sharedmassflow}}$

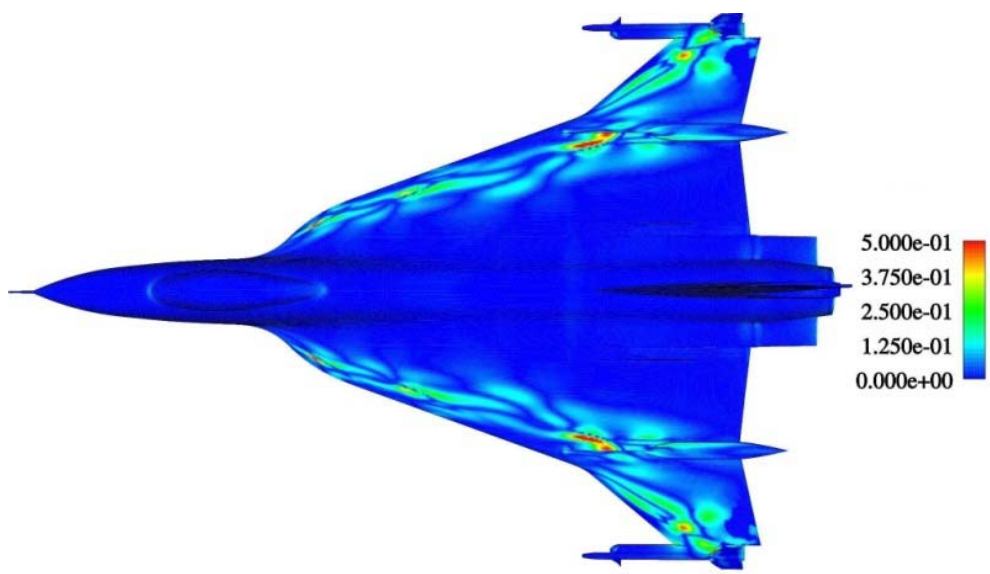

Figure 11-3: CAWAPI F-16XL-1, FC46, $C_{pBencmark} - C_{psharedmassflow}$.

The changes take place mostly along the leading edge and air dam, generally in areas where the pressure distribution is not flat but having large gradients and small change of solution is immediately visible. Figure 11-4 shows pressure distribution in butt lines for benchmark and on-line shearing setup calculations. Included is also a deviation of the pressure coefficient.

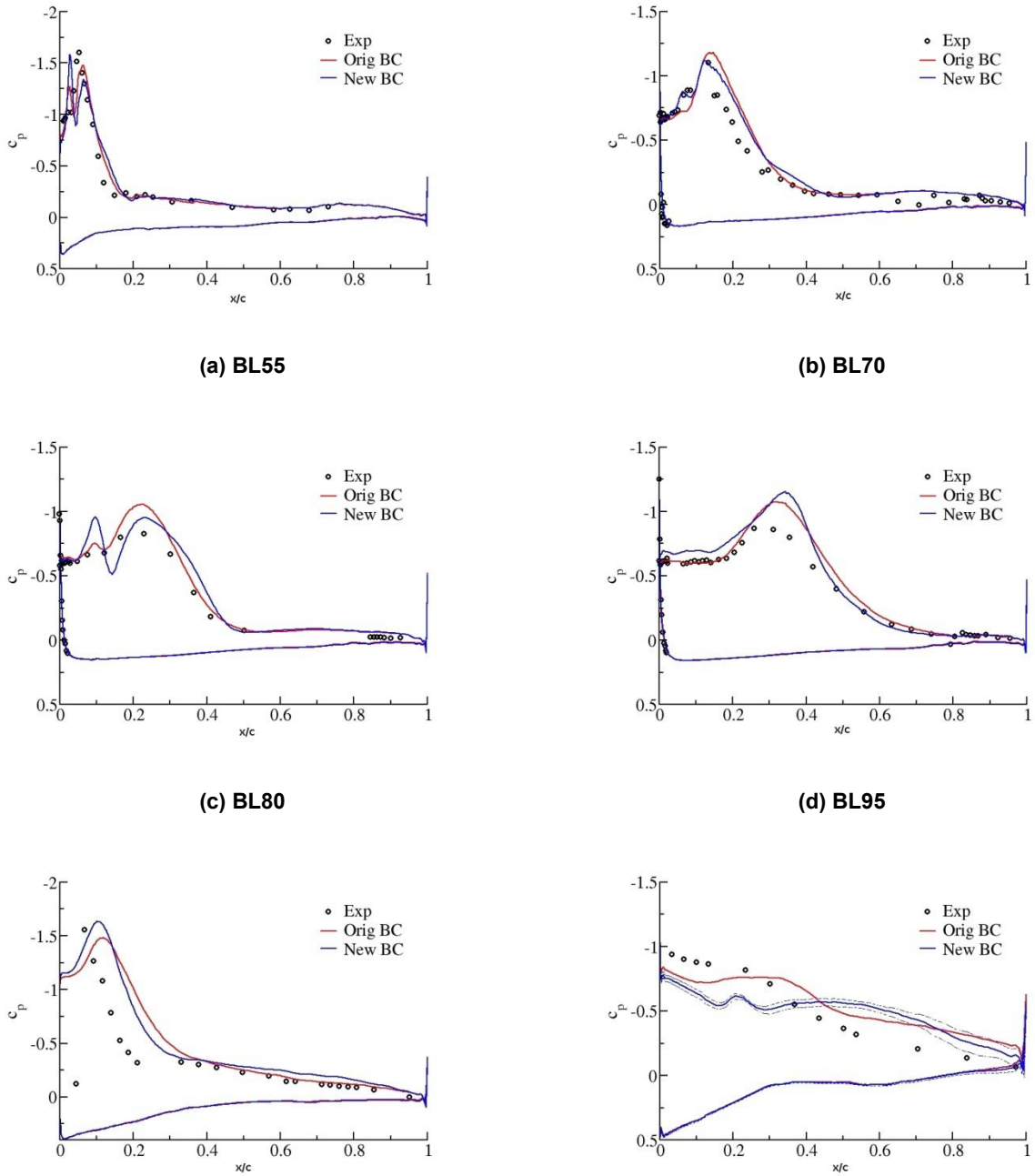

(a) BL55

(b) BL70

(c) BL80

(d) BL95

(e) BL153.5

(f) BL184.5

Figure 11-4: FC46, Chordwise Comparison of Computed and Measured Surface Pressure Coefficient along Six Butt-Lines (BL) for Case FC46: (a) BL55; (b) BL70; (c) BL80; (d) BL95; (e) BL153.5; and (f) BL184.5.

It is difficult to say which result is better. Note the rather large scatter of C_p data at BL 185 from on-line shearing setup. The question is what causes this kind of behaviour. The examination of the flow-field of the

on-line shearing setup revealed rather localised but intense flow separation behind the lower inlet lip – see Figure 11-5.

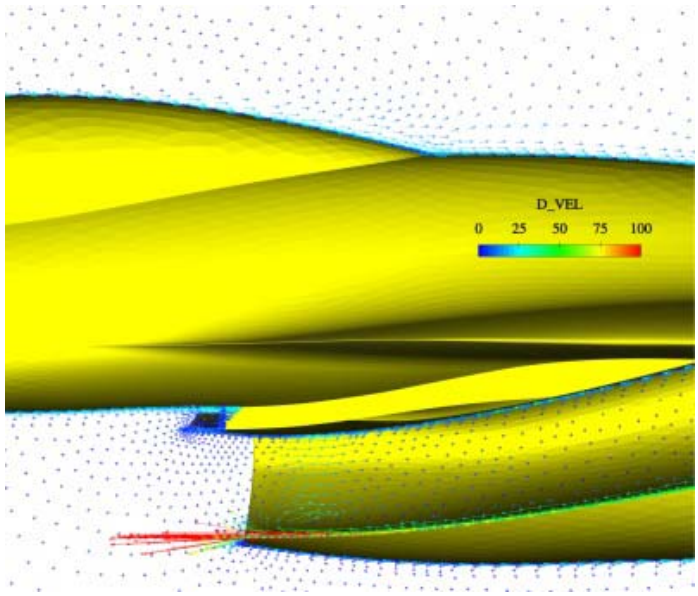

Figure 11-5: FC46, Velocity Vectors around Inlet Lips.

Apparently, this small but very intense spill-over makes the solution on the upper side change.

11.4.2.2 Flight Condition FC19

The analysis of flight conditions FC19 show similarity to previous flight conditions. The setup with online updated value of mass flow gave rise to flow separation behind the inlet lip with consequences to the pressure distribution on the upper side of the wing, as shown in Figure 11-6.

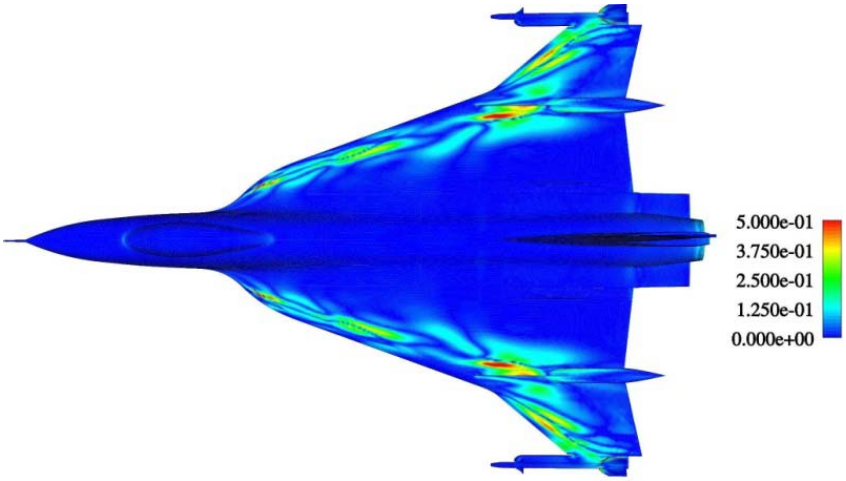

Figure 11-6: CAWAPI F-16XL-1, FC19, $C_{pBencmark} - C_{psharedmassflow}$.

Both C_p distribution and standard deviation of velocity show pretty much the same as in previous flight condition.

11.4.2.3 Flight Condition FC07

Unlike previous two cases, the flight condition FC07 does not show any dependency on different setup of boundary conditions. Detailed inspection of the figure revealed similar structure as in previous case – see Figure 11-7, however in order to visualize them the scale was updated. The largest difference in C_p between these two solutions is on the order of 0.05.

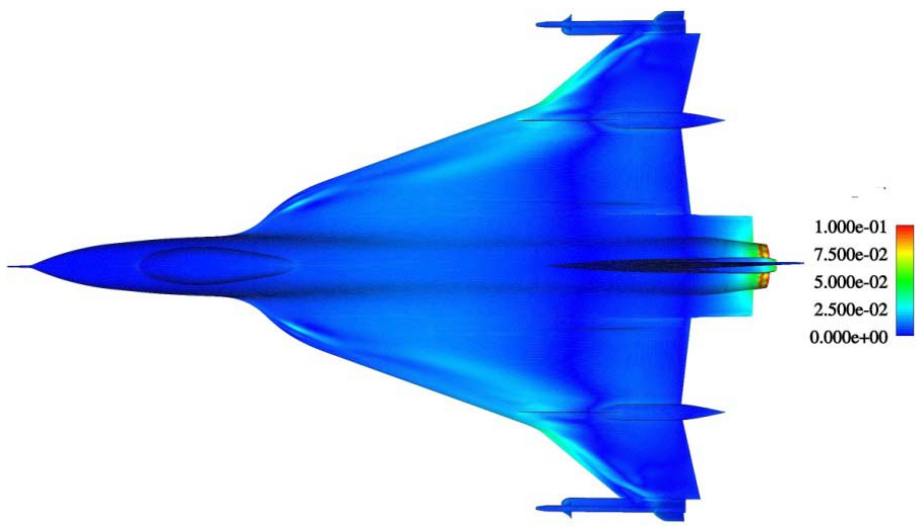

Figure 11-7: CAWAPI F-16XL-1, FC07, $C_{pBencmark} - C_{psharedmassflow}$.

11.4.3 Updated Values of Total Pressure in the Nozzle

Both on-line shearing setup and constant mass flow setup solutions were used to extract the value of total pressure at the mixing plane which is needed for balance of the mass flow through inlet and nozzle. The differences in values of the total pressure between these two setups are almost negligible. Table 11-2 shows these values.

Table 11-2: Values of Total Pressure in the Mixing Plane

FC	T_0 [K]	OMS P_0 [psia]	Corrected Value P_0 [psia]
FC07	583.3	23.0	14.17
FC19	583.3	21.5	11.39
FC46	580.6	14.8	8.86
FC25	671.7	21.5	12.99
FC70	666.7	21.5	9.48

As expected, the value of total pressure is substantially lower because the mass flow through the nozzle is lower. The inflow mass flow boundary condition which is used at the boundary in the mixing plane needs also the value of total temperature. This value is taken from Lamar et al. [11-1].

11.5 ADDITIONAL RESULTS

The inspection of the iso-surfaces of mean value and its deviation gives interesting figures. As an example, Figure 11-8 shows the iso-surface of the mean and its variance for entropy. Whilst the iso-surface of entropy in Figure 11-8 (a) shows several isolated vortices rising from the wing, the standard deviation of entropy shown in Figure 11-8 (b) shows more compact envelope of area including vortices.

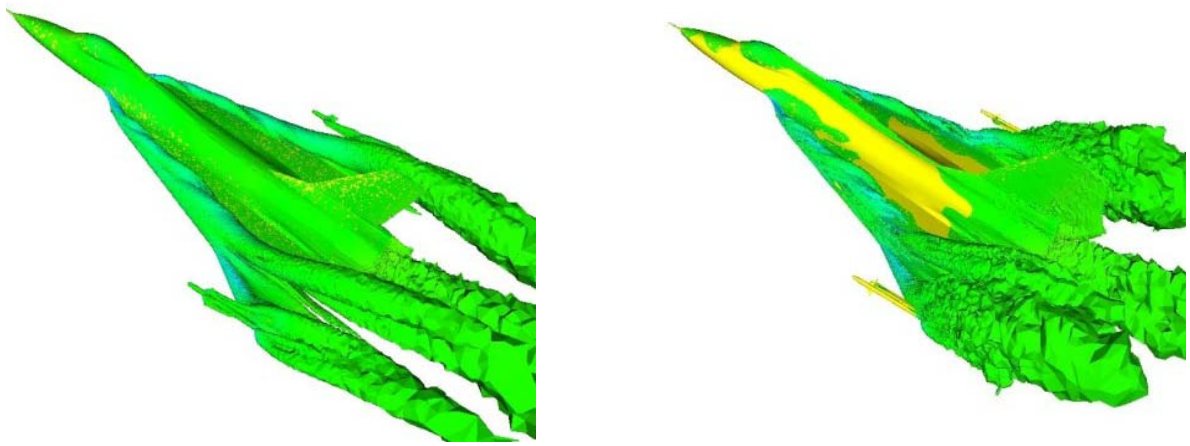

(a) Entropy – Mean Value **(b) Entropy – Deviation**

Figure 11-8: FC46, Iso-Surface of Entropy and its Standard Deviation.

Similar figures can be plotted for Mach number, total pressure or velocity – see Figure 11-9.

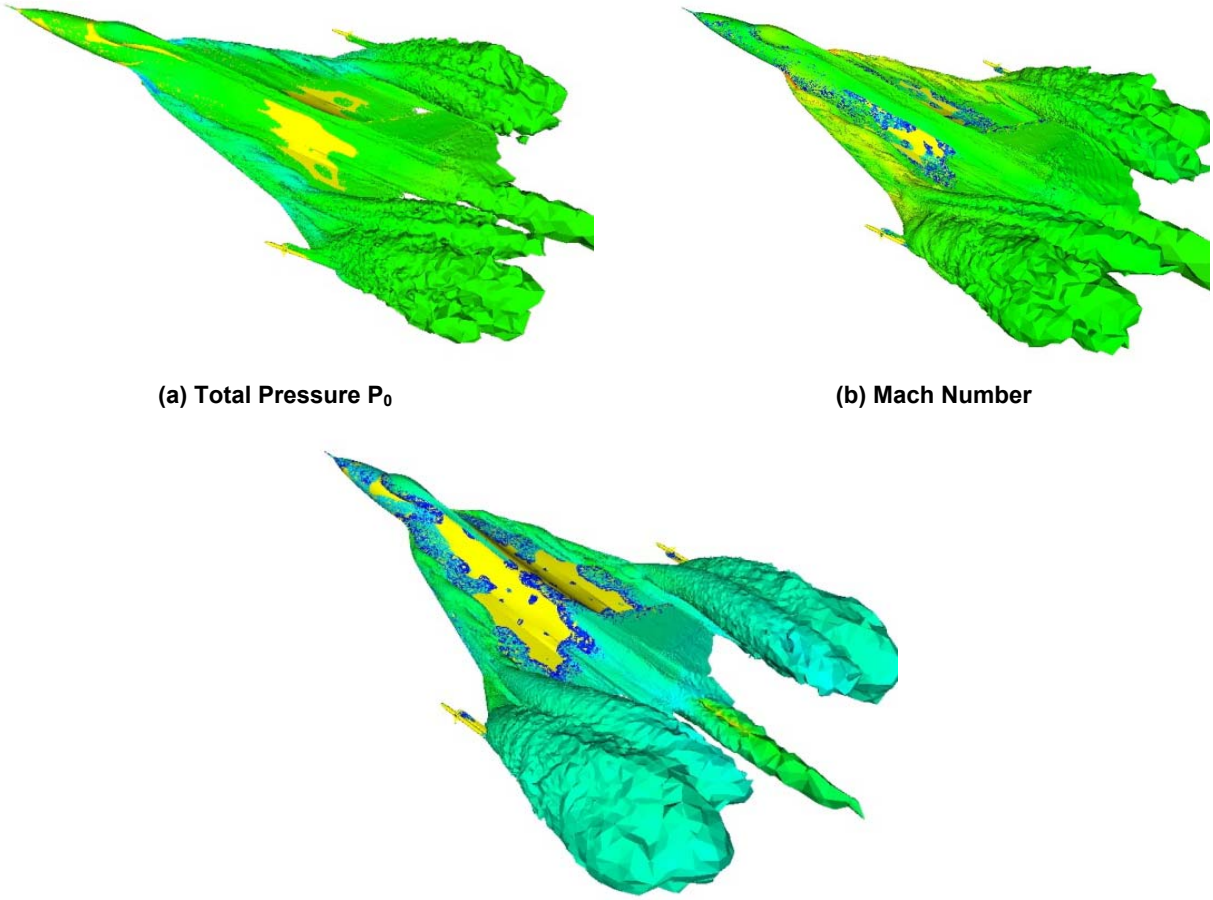

(a) Total Pressure P_0

(b) Mach Number

(c) Velocity

Figure 11-9: FC46, Iso-Surface for Standard Deviation of Total Pressure, Mach Number and Velocity.

What makes these figures interesting, particularly figures containing iso-surfaces of deviations is that they show very nicely vortical structure. It is also very easy to obtain such figures. It can be therefore expected that this approach can during mesh refinement for detecting areas where the flow structure may require improving of the computational mesh.

11.6 CONCLUSIONS

The standard boundary conditions at the inlet and the outflow from the nozzle used by all the CAWAPI participants were determined from a generic engine model. The exercise presented here focuses on the question of sensitivity of the formulation of these boundary conditions. Two approaches were chosen to determine alternative formulations to the standard one; the first is to keep the value of mass flow through the nozzle constant, and the second is to update the value of mass flow in the nozzle in every step of the computational process using the value of mass flow from the inlet. In both cases the total pressure in the nozzle are found to be substantially lower than that given by the formulation from the generic engine model. The first approach involves sharing the value of mass flow between the inlet and outlet boundaries and the mixing plane boundary in every step of the numerical process. It affects both solution and convergence of the numerical process at two

of the three flight conditions tested here. The most significant change in the solution takes place in the inlet where the flow is separated. This separation, whose extent is rather small, is intense and gives rise to changes of the flow around leading edge of the delta wing and consequently to the entire flow over the suction side of the wing. What cannot be answered is whether this observation is physically realistic or if it is just of a purely numerical nature.

The second approach, which simply corrects the value of mass flow through the inlet by prescribing its current-time value, had almost no effect on the flow around the wing. The only change occurred in the position of the shock on the outboard wing at the transonic flight condition. Rate of convergence of the computational process was the same as that of the benchmark case. In conclusion, although significant sensitivity was seen in one of the alternative formulations of the boundary conditions, there were not sufficient reasons to suggest that these conditions were better than the standard ones. Therefore the standard conditions have been used in CAWAPI.

11.7 ACKNOWLEDGEMENTS

The authors gratefully acknowledge the support provided by Lockheed Martin Aeronautics Company – Fort Worth in providing a refined IGES geometry file and the parameter values of a generic engine that were subsequently used by facet members in their CFD studies, and the geometrical work performed by Mr. Edward B. Parlette of Vigyan, Inc. in generating a series of unstructured, tetrahedral grids from the IGES file, with the last one known as the base grid. The authors gratefully acknowledge revisions of the document made by Dr. John Lamar. This work was financed by the Swedish Ministry of Defence and FOI. The financing is acknowledged.

11.8 REFERENCES

[11-1] Lamar, J.E., Obara, C.J., Fisher, B.D. and Fisher, D.F.: *Flight, Wind-Tunnel, and Computational Fluid Dynamics Comparison for Cranked Arrow Wing (F-16XL-1) at Subsonic and Transonic Speeds*, NASA/TP 2001-210629, NASA, February 2001.

[11-2] Lamar, J.E. and Obara, C.J.: *Review of Cranked-Arrow Wing Aerodynamics Project: Its International Aeronautical Community Role*, AIAA Paper 2007-0487, Presented at 45th AIAA Aerospace Sciences Meeting and Exhibit, Reno, NV, January 8-11 2007.

[11-3] Görtz, S. and Jirásek, A.: *Chapter 10 – Numerical Solutions for the CAWAPI Configuration on Unstructured Grids at KTH/FOI – Part I*, RTO-TR-AVT-113, 2009.

[11-4] Morton, S.A., McDaniels, D.R. and Cummings, R.M.: *F-16XL Unsteady Simulations for the CAWAPI Facet of RTO Task Group AVT-113*, AIAA Paper 2007-0493, Presented at 45th AIAA Aerospace Sciences Meeting and Exhibit, Reno, NV, January 8-11 2007.

[11-5] Eliasson, P.: *EDGE, a Navier-Stokes Solver for Unstructured Grids*, Proc. to Finite Volumes for Complex Applications III, ISBN 1 9039 9634 1, 2002, pp. 527-534.

[11-6] Hellsten, A.: *New Advanced k-ω Turbulence Model for High Lift Aerodynamics*, AIAA Journal, Vol. 43, No. 9, 2005.

[11-7] Jirásek, A.: *Mass Flow Boundary Conditions for Subsonic Inflow and Outflow Boundary*, AIAA Journal, Vol. 44, No. 5, May 2006.